Published in final edited form as:
*J Theor Biol*. 2013 July 7; 328: . doi:10.1016/j.jtbi.2013.03.008.

# Computational modeling of tuberculous meningitis reveals an important role for tumor necrosis factor-α

**M. El-Kebir**[a,b,c,d,*], **M. van der Kuip**[a,*], **A.M. van Furth**[a], and **D.E. Kirschner**[d]

[a]Department of Pediatric Infectious diseases and Immunology, VU University Medical Center, Amsterdam, the Netherlands [b]Centrum Wiskunde & Informatica, Life Sciences Group, Amsterdam, the Netherlands [c]Centre for Integrative Bioinformatics VU, VU University Amsterdam, the Netherlands [d]Department of Microbiology and Immunology, University of Michigan, Ann Arbor, MI 48109, USA

## Abstract

Tuberculosis is a global health issue with annually about 1.5 million deaths and 2 billion infected people worldwide. Extra pulmonary tuberculosis comprises 13% of all cases of which tuberculous meningitis is the most severe. It has a high mortality and is often diagnosed once irreversible neurological damage has already occurred. Development of diagnostic and treatment strategies requires a thorough understanding of the pathogenesis of tuberculous meningitis. This disease is characterized by the formation of a cerebral granuloma, which is a collection of immune cells that attempt to immunologically restrain, and physically contain bacteria. The cytokine tumor necrosis factor-α is known for its important role in granuloma formation. Because traditional experimental animal studies exploring tuberculous meningitis are difficult and expensive, another approach is needed to begin to address this important and significant disease outcome. Here, we present an *in silico* model capturing the unique immunological environment of the brain that allows us to study the key mechanisms driving granuloma formation in time. Uncertainty and sensitivity analysis reveal a dose-dependent effect of tumor necrosis factor-α on bacterial load and immune cell numbers thereby influencing the onset of tuberculous meningitis. Insufficient levels result in bacterial overgrowth, whereas high levels lead to uncontrolled inflammation being detrimental to the host. These findings have important implications for the development of immuno-modulating treatment strategies for tuberculous meningitis.

### Keywords

Agent based model; Central nervous system; Extrapulmonary tuberculosis; Granuloma formation; Meninges; Rich focus; Tumor necrosis factor

## 1. Introduction

Tuberculosis (TB) is a global health issue. One third of the world population is infected with *Mycobacterium tuberculosis* (Mtb) and each year 9 million people develop disease [1]. TB



*Joint first authorship

is the second leading killer after human immunodeficiency virus with annually about 1.5 million deaths; ten percent of whom are younger than 15 years old [1, 2]. Therefore the reduction of prevalence and death rates, and improvement of detection and treatment strategies is one of the United Nation's 2015 millennium development goals [3].

Mtb is a slow-growing microorganism with a doubling time of 1 to 4 days [4]. It is a highly infectious pathogen and aerosol transmitted. Inhalation of a single droplet containing just a few bacteria can lead to pulmonary infection [5, 6]. From a local pulmonary focus of TB, bacilli can disseminate through lymphatic or blood vessels and lead to extra pulmonary TB [7]. Of the 6.2 million reported TB disease cases in 2010, 790,000 (13%) patients had extra pulmonary TB [7]. Especially individuals with immature or impaired immune function such as young children and HIV patients are more likely to develop extra pulmonary TB [8, 9, 10]. Tuberculous meningitis (TBM) is the most severe form of extra pulmonary TB and occurs in 0.5–3 percent of all TB cases [11]. The development of TBM usually starts insidiously with a period of nonspecific symptoms, such as fever, malaise and behavioral changes. As the disease progresses, neck stiffness, loss of consciousness, motor paresis and convulsions will follow. Often TBM is diagnosed once irreversible neurological damage has already occurred and the mortality is high [12].

There is a large discrepancy between the number of infected people (in the order of billions) and the number of annual deaths (in the order of millions). This discrepancy points to an important fact about TB: not all infected people progress to active disease, rather most individuals achieve a latent state and while they are in this state they do not show clinical symptoms of disease nor are they able to infect others. The formation of a granuloma, guided by several cytokines and chemokines, plays an important role in achieving this latency [13]. A granuloma is a spherical accumulation with a characteristic spatial pattern consisting of a necrotic caseating core with bacteria, surrounded by several types of immune cells as shown in Figure 1.

The existence of cerebral granuloma was shown in 1933 by post-mortem pathology studies of Rich and McCordock [14]. In their meticulous work the authors demonstrated that the majority of TBM patients displayed a caseating focus in the brain parenchyma or the meninges. The authors postulated that these cerebral granuloma, also termed "Rich foci", develop around blood-borne bacteria deposited in the meninges and brain parenchyma. The rupture of these Rich foci to the meninges leads to meningitis.

Although valuable to understanding morphological aspects of TBM, postmortem pathology studies do not provide insights in the dynamics of host-pathogen interactions of granuloma formation and function during TB. Instead, they only provide a snapshot in time of the dynamic events occurring during a progressive infection occurring over weeks to months. To study the dynamics of TBM, several animal models ranging from mouse, guinea pig, rabbit and pig, have been used [11]. Specifically, the role of the cytokine tumor necrosis factor-$\alpha$ (TNF-$\alpha$) was addressed by Tsenova et al. [15]. In a rabbit model they observed that cerebral infection leads to elevated TNF-$\alpha$ levels. More recently, the role of TNF-$\alpha$ was studied in zebrafish and humans [16, 17, 18]. In addition to animal models, several *in vitro* models have been developed [11, 19]. For instance, Jain et al. used a monolayer of primary human brain microvascular endothelial cells to study the translocation of Mtb across the blood brain barrier [20] (explained in next section, Figure 2a).

Both the *in vitro* and animal models are useful for studying host-pathogen interactions but are insufficient to study the dynamics of granuloma development. This is mainly due to the low growth rate of mycobacteria, requiring experiments ranging from weeks to months. An additional approach to aiding currently experimental investigations is an *in silico* model

capable of studying host-pathogen interactions in time. In order to model the immune response to Mtb, weneed to have an *in silico* modeling method that captures the interplay in a bottom-up fashion starting from the individual parts — immune cells, Mtb, cytokines and chemokines — and resulting in the expected emergent behavior — the formation of a granuloma. Previously, we used *in silico* models to show that the levels, functions and gradients of the cytokine TNF-$\alpha$ in a pulmonary TB granuloma are critical to granuloma structure and function [21, 22, 23]. In this work, we introduce a novel *in silico* model capturing the immune response to Mtb in the brain. Using this model, we study the effects of TNF-$\alpha$ on cerebral granuloma formation in TBM. We test the hypothesis that there is a dose-dependent effect of TNF-$\alpha$ on bacterial load and thereby the onset of TBM. In addition, we test the extent that the degree of cerebral vascularization has an effect on TBM development.

## 2. Immunobiology of TBM

The central nervous system (CNS) is comprised of the brain and the spinal cord, which are enveloped by meninges. The primary function of the meninges is to offer protection to the CNS. Meninges comprise three layers: the dura mater, the arachnoid mater and the pia mater Figure 2a. In the subarachnoid space, the space between the arachnoid mater and the pia mater, cerebrospinal fluid (CSF) is present. CSF provides mechanical and immunological protection to the brain. Meningitis is defined by inflammation of the meninges and CSF. The cerebral cortex, the outer layer of the brain, is highly vascularized with a vascular volume of roughly 2% of the total volume [24]. Impaired cerebral blood circulation and its clinical consequences is a major feature of TBM. Cerebral vasculitis, inflammation of cerebral blood vessel walls, leads to thrombosis (obstruction by a blood clot). Thrombosis leads to stroke, which is characterized by tissue damage due to lack of oxygen and nutrients in downstream tissue.

The blood-brain barrier (BBB) separates the CNS from the regular systemic blood circulation (Figure 2a). In addition, unlike other organs the CNS lacks a draining lymph node. For these reasons, the CNS used to be thought of as an immunologically privileged area, i.e. an area where no inflammatory immune response takes place upon the introduction of antigen. Recent studies indicate that this view is not correct. Both immune cells from outside the CNS that cross the intact BBB and resident brain phagocytes, participate actively in immune responses in the CNS [25, 26].

### 2.1. Immune cells and cytokines

Two types of phagocytes reside in the brain: macrophages and microglia. Macrophages are predominantly present in the meninges and around blood vessels [27] and have a life span of 100 days [28]. Unlike macrophages, which occur ubiquitously throughout the body, microglia only occur in the brain. The fundamental characteristic of microglia is plasticity: based on their ability to change shape and to their capacity to up or down regulate their functional activities. In the literature three states are distinguished in microglia: ramified, reactivated and amoeboid [29, 30]. The microglia population consists of mainly ramified microglia, which have a small cell body (5–10 $\mu$m) and thin branching dendrites. Ramified microglia are involved in immunosurveillance and regain their phagocytic abilities by becoming reactive following inflammation or infection [31]. Amoeboid microglia are only present during fetal brain development. Both macrophages and microglia have the ability to secrete chemokines such as CCL2, CCL5, CXCL9/10/11 [29, 30, 32], which play a role in the movement and recruitment of other immune cells.

Macrophages and microglia ingest mycobacteria by receptor-assisted phagocytosis mediated by several distinct cell surface molecules. A phagocyte will try to kill an ingested pathogen

by fusing the phagosome with a lysosome containing toxic chemicals such as nitric oxide (NO). Although Mtb has developed several survival mechanisms to avoid fusion and killing by intracellular toxins [33], activated phagocytes are able to kill intracellular and extracellular Mtb. In the activated state the two transcription factors NF$\kappa$B and STAT1 are expressed, which play a role in the signaling pathway leading to NO production [34]. The transcription factor NF$\kappa$B is induced by bacterial antigens or TNF-$\alpha$. The NF$\kappa$B signaling pathway augments chemokine and cytokine expression thereby enhancing immune cell recruitment to the site of infection. Moreover, if a phagocyte is able to kill mycobacteria, mycobacterial antigens will be presented to CD4+ T lymphocytes, inducing further adaptive immune surveillance. Three functional types of T cells play an important role in the pathogenesis of TBM: IFN-$\gamma$ secreting T cells ($T_\gamma$), cytotoxic T cells ($T_{\text{cyt}}$) and regulatory T cells ($T_{\text{reg}}$). $T_\gamma$ cells comprise both CD4+ and CD8+ T cells that secrete IFN-$\gamma$ and thus are able to activate phagocytes. In addition to playing a crucial role in the activation of macrophages and microglia through the transcription factor STAT1, $T_\gamma$ cells have the ability to induce Fas/FasL apoptosis in infected phagocytes. $T_{\text{cyt}}$ cells correspond to CD8+ cytotoxic T cells. $T_{\text{reg}}$ cells are responsible for down-regulating the immune response [35].

### 2.2. The specific role ofTNF-$\alpha$ in granuloma formation

TNF-$\alpha$ has four main actions during TB. It plays a key role in (1) activation of macrophages, affecting their phagocytic and killing abilities; (2) recruitment of many inflammatory cells (key for proper granuloma formation); (3) induction of cytokine and chemokine production; and (4) induction of apoptosis of macrophages and T cells [36]. TNF-$\alpha$ is known to play an important role in granuloma development. Murine data suggest that TNF-$\alpha$ is essential to the formation, structure and maintenance of a granuloma: TNF-$\alpha$-deficient mice have increased susceptibility to tuberculosis and develop poorly-structured granuloma with many bacteria [37]. Similar results have been shown in nonhuman primates [38, 39]. Also, humans treated with TNF-$\alpha$-neutralizing drugs show increased incidence of TB reactivation [40] and subsequent granuloma development [41].

Very recently the underlying mechanism of TB susceptibility in both zebrafish and humans were studied [16, 17]. Through the protein leukotriene A4 hydrolase encoded by LTA4H, the balance between pro-, and anti-inflammatory response is regulated. Individuals with a specific mutation on both alleles of the gene LTA4H develop an anti-inflammatory response with little TNF-$\alpha$ production, whereas individuals having two wild-type alleles have a pro-inflammatory phenotype with abundant TNF-$\alpha$ levels. Both cases are detrimental to the host leading to bacterial overgrowth and hyperinflammation, respectively. On the other hand, intermediate TNF-$\alpha$ levels, as seen in individuals heterozygous for LTA4H, result in moderate inflammation, controlled infection and low risk of severe disease or death [16].

## 3. Materials and methods

### 3.1. Model description

A modeling method specifically tailored toward modeling complex systems such as the immune system is agent-based modeling [42]. An agent-based model (ABM) consists of (1) a predefined environment on which (2) autonomous agents reside and (3) behave according to a set of rules which are performed for (4) a given time scale. This is in contrast to traditional differential equations models in which agents are assumed to be part of homogeneous populations represented by continuous variables and where interactions take place on the population level and are inherently deterministic. Our model is based on an existing pulmonary agent-based model for TB [21] and tailored to the immunological environment of the brain. We will describe our model by considering the four main components that make up an ABM. More details are given in Supplementary Text 1.

**3.1.1. Environment—**We work with a 2-dimensional (2-D) model framework as data provided from granulomas in lung and brain are 2-D histology sections and we can reproduce those data in an easy fashion. This also provides computational efficiency, as 3-D models are computationally intensive. The environment is a cross-section of 2 mm × 2 mm of cerebral cortex, subdivided by micro-compartments. The size of a micro-compartment is chosen to be the same as that of a macrophage, namely 20 $\mu$m × 20 $\mu$m. The uniform grid is thus comprised of 100 × 100 micro-compartments. There can be at most two immune cells present in a micro-compartment. Should one of those be a phagocyte, then it can only be accompanied by a T cell. We include meninges in the environment by defining one edge of the grid to correspond to meninges, whereas the other three edges correspond to brain tissue. Since the edges correspond to different types of tissue, the grid is not toroidal as was done previously [21]. Instead, as soon as an immune cells moves out of the grid, it is removed from the grid. The 2% vascular volume of the cerebral cortex amounts to 200 sources out of 10,000 micro-compartments. Recruitment of new immune cells is through vascular sources, while proliferation of microglia occurs on site. Micro-compartments can become caseated over time, at which point they become inaccessible for immune cells. Immune cells can move to non-caseous micro-compartments guided by a chemokine gradient (chemotaxis). For every micro-compartment we keep track of the levels of the cytokine TNF-$\alpha$ and the chemokines CCL2, CCL5 and CXCL9/10/11. In addition, we consider the cytokine IFN-$\gamma$ by means of IFN-$\gamma$ producing T cells, as IFN-$\gamma$ is secreted in a very localized way, rather than more diffuse and larger amounts, such as TNF-$\alpha$ and chemokines. In Figure 2b an example grid illustrating the described concepts is given.

**3.1.2. Model agents—**The agents in our model correspond to mycobacteria and immune cells that can be in different states of behavior. An immune cell changes state due to intrinsic factors or interactions with its direct neighborhood. An example of an intrinsic factor is cell death due to age. Cell death can also occur due to apoptosis induced by TNF-$\alpha$, which is the result of interaction with the environment.

**Mycobacterium tuberculosis:** In our model we use an intracellular doubling time of 75 hours of Mtb. Since Mtb prefers the intracellular environment of phagocytes over the extracellular environment, we use a longer extracellular doubling time of 150 hours [21]. Due to limited resources (nutrients) and space, a micro-compartment can only accommodate up to 200 extracellular bacteria [4]. Since Mtb are non-motile, we assume that bacteria do not diffuse.

### Phagocytes

***Cell types and states:*** In our model we consider two types of phagocytes: macrophages and microglia. Unlike for macrophages, the average lifespan of microglia is unknown [43], but turnover computations yield a lifespan of up to 1000 days [44]. Similar to macrophages, we use a 100 day lifespan for microglia. Both types of phagocytes may contain intracellular bacteria and assume one of the following states: resting, infected, chronically infected and active. Initially, microglia are in the ramified state. In addition to the states, we consider the two transcription factors NF$\kappa$B and STAT1 [45].

***State transitions:*** Figure 3 shows state transitions of macrophages and microglia, which we will describe in the following. Initially, a newly recruited or proliferated phagocyte is in the resting state. Upon encountering extracellular Mtb, a resting phagocyte may become infected depending on the load. In case of a single bacterium, the phagocyte will kill it and remain resting otherwise the phagocyte may become infected. If both NF$\kappa$B and STAT1 are enabled, a resting or infected phagocyte becomes active. In the active state, a phagocyte is able to kill extracellular Mtb at the cost of a reduced lifespan of 10 days. Intracellular Mtb

within an infected phagocyte proliferate. When the intracellular bacterial load exceeds a threshold (5 for microglia and 10 for macrophages), the phagocyte becomes chronically infected. At this point the bacteria will continue to proliferate until the phagocyte bursts and releases its load. Specifically, a chronically infected macrophage bursts when more than 20 intracellular mycobacteria are present, whereas a microglial cell bursts at a threshold of 10 bacteria. In case a (chronically) infected phagocyte dies of age, its intracellular bacteria are released into the neighboring micro-compartments. If the phagocyte is in the active state, its death will contribute to caseation. In contrast to death by aging, TNF-$\alpha$-induced apoptosis of (chronically) infected phagocytes results in the death of half of the intracellular bacteria and dispersion over the Moore neighborhood of the other half. Reactive microglia encompass the following four states: resting, infected, chronically infected or activated. A ramified microglial cell becomes resting [46] if the TNF-$\alpha$ concentrations exceeds a predefined threshold, which is a model parameter that we can explore with uncertainty and sensitivity analysis. On the other hand, it may become infected by uptaking extracellular bacteria in the Moore neighborhood [46].

***Movement and secretion of chemokines/cytokines:*** Phagocytes move from one micro-compartment to a neighboring compartment via a chemokine gradient. The higher the gradient in a neighboring micro-compartment, the more likely the phagocyte moves onto that compartment. A ramified microglial cell is stationary. Chemotaxis by macrophages and reactive microglia is dependent on CCL2 and CCL5 [31]. Since we only consider a small cross-section of brain parenchyma, the model allows cells to move off the grid. Meningeal macrophages cannot move from the meninges to the brain parenchyma, but they can move off the grid. The speed by which phagocytes move depends on their state. For instance, chronically infected phagocytes do not move at all. Whereas resting, infected and active phagocytes move at different velocities. Both macrophages and microglia have the ability to secrete the chemokines CCL2, CCL5, CXCL9/10/11 and the cytokine TNF-$\alpha$ [29, 32, 30, 31]. Secretion is dependent on the transcription factor NF$\kappa$B and the state of the phagocyte. For instance, ramified microglia do not secrete at all, whereas resting phagocytes that have NF$\kappa$B enabled secrete at half rate. In all other cases where NF$\kappa$B is enabled, secretion happens at maximal rate. Infected phagocyte secrete at half rate if NF$\kappa$B is disabled.

***Recruitment and proliferation:*** Macrophage recruitment at vascular sources depends on TNF-$\alpha$, CCL2 and CCL5. We maintain a steady-state population of meningeal macrophages through recruitment via vascular sources in the meninges. Unlike the other immune cells, microglia are not recruited through vascular sources. Rather they reside and proliferate on site. We make a distinction between proliferation rates for ramified and reactivated microglia with ramified microglia dividing at a slower rate than reactive microglia [47]. Continuous proliferation serves to maintain a steady-state population of ramified microglia. We allow only activated and resting microglia to proliferate depending on TNF-$\alpha$, CCL2 and CCL5. Proliferation of a reactive microglial cell results in the creation of a new resting microglial cell with both NF$\kappa$B and STAT1 turned off.

## T lymphocytes

***Cell types and states:*** In the model we consider the three functional T cell types as mentioned earlier: $T_\gamma$, $T_{\text{cyt}}$ and $T_{\text{reg}}$. Since IFN-$\gamma$ is directly secreted into the immunological synapse of the phagocytes [48], we do not consider it as a separate cytokine but use $T_\gamma$ cells as a proxy. The cytokine interleukin-10 (IL-10) is responsible for the down-regulatory function of $T_{\text{reg}}$ cells [35] and is also secreted directly into the immunological synapse [48]. Therefore, we use $T_{\text{reg}}$ cells as a proxy for IL-10. Both $T_\gamma$ and $T_{\text{cyt}}$ can be in the following states: active or down-regulated. A $T_{\text{reg}}$ cell has only one state in which it down-regulates every immune cell in its Moore neighborhood. A down-regulated immune cell is able to

move on the grid but it does not interact with its environment nor does it secrete chemokines and cytokines. In addition, if the immune cell is a phagocyte then its transcription factor STAT1 is switched off upon down-regulation.

***State transitions:*** When a $T_{cyt}$ is down-regulated by a $T_{reg}$ cell, it does not perform its cytotoxic activities for a predefined number of time steps. In the active state, the cytotoxic activities of a $T_{cyt}$ cell consist of killing infected or chronically infected phagocytes in its local micro-compartment. Death of a chronically infected phagocyte has two possible outcomes: either it is killed totally and none of its intracellular bacteria are dispersed, or the killing results in the dispersion of all intracellular bacteria over the Moore neighborhood. Cytotoxic killing of a phagocyte contributes to caseation. In addition to playing a crucial role in the activation of macrophages and microglia through the transcription factor STAT1, $T_\gamma$ cells have the ability to induce Fas/FasL apoptosis in (chronically) infected phagocytes. This results in the dispersion of half of the intracellular bacteria over the Moore neighborhood. Unlike TNF-$\alpha$-induced apoptosis, apoptosis due to the Fas/FasL pathway does contribute to caseation. If a $T_\gamma$ cell is down-regulated, it does not induce apoptosis for a pre-defined period nor is it able to activate the STAT1 pathway.

***Movement and secretion of TNF-α:*** Similar to phagocytes, movement of T cells is dependent on the chemokine levels. Specifically, movement of $T_\gamma$ cell depends on CCL2, CCL5 and CXCL9/10/11, $T_{cyt}$ cells depend on CCL5 and CXCL9/10/11 and $T_{reg}$ cells on CCL5 only [21]. Active $T_\gamma$ and $T_{cyt}$ secrete TNF-$\alpha$. As previously mentioned, a micro-compartment may contain up to two immune cells. The probability of a T cell moving onto a micro-compartment already containing a phagocyte is parameter of our model.

***Recruitment:*** $T_\gamma$ and $T_{cyt}$ cells are recruited at vascular sources by taking the levels of TNF-$\alpha$, CCL2, CCL5, CXCL9/10/11 into account. Recruitment of $T_{reg}$ cells is dependent on TNF-$\alpha$ and CCL5 only.

**3.1.3. Model initialization and time scales—**The model is initialized by placing the initial inoculum consisting of one macrophage infected with an intracellular bacterium on the grid. In addition, initial populations of resting uninfected phagocytes are placed on the grid as well. The final step is to initialize the static elements of the environment by randomly placing the 200 vascular sources on the grid as well as making the micro-compartments on the right edge part of the meninges.

The ABM is run for 200 days by executing 28,800 10-minute time steps. The first step of the main loop concerns the secretion, diffusion and degradation of chemokines and cytokines. This happens at a finer timescale of 6-second time steps. Subsequently, all microglia are moved followed by moving macrophages and then T cells. After that, microglial cells proliferate and new immune cells are recruited. Then the immune cell specific rules are performed, and the growth function of extracellular Mtb is applied. These computational updates occur in an asynchronous manner.

### 3.2. Model implementation

This section gives a brief overview of the implementation details of the developed sofware. For a more detailed description see [49]. The complexity of our ABM, due to cell numbers, interactions and time scales, requires an efficient implementation. Therefore, we chose to implement our model in C++. In order for our software to be cross-platform among Linux, Windows and MacOS X, we made use of the Qt framework (Nokia, 2010). Qt is a framework for developing cross-platform applications with a graphical user interface (GUI). We implemented various visualization techniques including color mapping, isolines, height

plots and agent visualization using OpenGL (Khronos, 2010). Through the GUI, the user is able to zoom in on a specic part of the grid, inspect the contents of a particular micro-compartment and also view simulation-wide attributes and statistics in real-time. All of this proceeds without any observable delays while the simulation is running. The software also allows the user to save and load model states and alter parameters, enabling the user to perform depletion experiments regarding a particular cytokine or chemokine. The software is freely available on http://malthus.micro.med.umich.edu/lab/movies/TBM/.

### 3.3. Model validation

We validate our model in four consecutive steps, which will be described in the following sections in more detail. First, an extensive exploration of the parameter space is performed by means of an uncertainty analysis. Next, we identify key parameters in our model using a sensitivity analysis. A correct model is expected to recapitulate the three typical TB outcomes of containment, clearance and dissemination on the granuloma level. As the third step, we screen the resulting experiments for all these outcome scenarios identifying baseline parameter sets for the three scenarios. The final step consists of additional experiments corresponding to virtual depletions of several parameters on the containment baseline parameter set, which allow us to uncover key mechanisms driving TBM.

**3.3.1. Parameter estimation — uncertainty analysis—**There are 44 parameters in the model, 16 of which have values from the literature. These values are estimated from *in silico, in vitro* or *in vivo* experiments where the latter can be both animal or human studies. When assigning the unknown parameters different values, different model outputs may result. In addition to *epistemic* uncertainty due to missing parameters values, we also have *aleotory* uncertainty as a result of stochasticity. In order to deal with these two types of uncertainty, we use the Latin Hypercube Sampling (LHS) method [50]. We vary 24 parameters, which are sampled within their individual ranges after dividing them into 500 subranges with 5 repetitions per sample (see Table 1). Supplemental Table 1 contains the complete list of model parameters including their values and ranges when varied during the LHS; if not varied, an estimated value together with a reference is given.

**3.3.2. Uncovering key mechanisms — sensitivity analysis—**To determine the extent to which variations in input parameters lead to different model outcomes, we use a sensitivity analysis as described by Marino et al. [50]. Here, the model outcome of interest is the onset of meningitis which we approximate with the bacterial load (the sum of intra- and extracellular bacteria). We use partial rank correlation coefficients (PRCC) to quantify the relation between bacterial load and model parameters. PRCC values are between −1 and 1. A value of −1 corresponds to perfect negative correlation, whereas +1 is perfect positive correlation. PRCCs can be tested to be different from 0 using Student's $t$ test. Here, we use a significance level of 0.0001 corresponding to PRCC values above 0.21 or below −0.21.

**3.3.3. Baseline identification—**Among the 2,500 experiments performed in the LHS, the simulation outcomes could be classified as clearance (no bacterial load), containment (low bacterial load stable over time) and dissemination (high and continuously increasing bacterial load). These outcomes hold true on an individual granuloma basis and not on a host/entire brain scale. We quantitatively identified a containment parameter set by specifically requiring low (a load of less than 500 bacteria), stable (a coefficient of variation below 20%) and mostly intracellular bacterial load (ratio of extracellular versus intracellular Mtb at most 10%) from days 100 to 200. Screenshots of the grid at days 50, 100, 150 and 200 (as shown in Figure 6b) were generated to visually assess and confirm a containment scenario. Supplemental Table 1 shows the parameter values corresponding to the containment scenario.

**3.3.4. Identifying the effect of key mechanisms—**Using the previously identified baseline containment scenario, we can study the effect of any individual parameter by means of a virtual depletion experiment which mimics an experimental gene-knockout studies. We do this by varying the parameter's value while keeping the other parameters fixed. We use this technique to study the effect of the parameter that is most correlated with model outcome. In addition, we study the effect of vascularization on model outcome as well as the effect of the delay in T cell recruitment.

## 4. Results

### 4.1. Key mechanisms in Rich focus formation

In Table 1, we show the association between bacterial load and parameter values that have been varied in the uncertainty analysis. Using a $z$ test, we found that the secretion rate of TNF-$\alpha$ was the most important mechanism on bacterial load compared to the other parameters (with $p$ values less than 0.059, see Supplemental Table 2. In the next subsection we will elaborate on the effect of this parameter on granuloma outcome.

Several parameters associated with adaptive immunity were shown to be significantly correlated with the bacterial load. These parameters were the recruitment probability of T cells through vascular sources ($p_{\mathrm{T,recr}}$) and their subsequent penetration into the granuloma core ($p_{\mathrm{T,P}}$ and $p_{\mathrm{T,T}}$). These parameters as well as the role of caseation ($N_{\mathrm{caseous}}$) will not be further studied in this paper.

However, T cell recruitment ($p_{\mathrm{T,recr}}$) reflects another crucial aspect of granuloma formation. Together with phagocyte recruitment ($p_{\mathrm{M,recr}}$) it emphasizes the role of vascularization. From a clinical point of view, diminished vascularization is caused by vasculitis and infarction during TBM development. In Subsection 4.3 we will study the role of vascularization on model outcome.

### 4.2. The importance of TNF-α on granuloma outcome

Using a baseline containment scenario and varying the TNF-$\alpha$ secretion rate while keeping the other parameters fixed at baseline levels list in Supplementary Table 1, we determined a dose-dependent response of TNF-$\alpha$ secretion rate on bacterial load and immune cell numbers. Figure 5 shows that (1) low TNF-$\alpha$ levels result in bacterial overgrowth, (2) high TNF-$\alpha$ levels result in hyperinflammation and (3) an intermediate TNF-$\alpha$ secretion rate leads to a balance between infection and inflammation characterized by containment or even clearance of Mtb. Figure 6 depicts these three TNF-$\alpha$ secretion levels and their corresponding granulomas at days 50 and 200. There low levels of TNF-$\alpha$ lead to uncontrolled growth of Mtb. Conversely, a high dose of TNF-$\alpha$ results in clearance of Mtb but at the cost of hyperinflammation leading to tissue damage. Intermediate TNF-$\alpha$ levels lead to the formation of a stable granuloma controlling the infection at that site.

### 4.3. The role of vascularization in TBM

To study the effect of vascularization on bacterial load and immune cell numbers, we varied the number of vascular sources from an ischemic (inadequate flow of blood) to a hyperemic state (increased blood flow) by sampling $N_{\mathrm{sources}}$ from 1 to 500 while keeping the other parameters the same as in the baseline containment scenario (Figures 7 and 8). A low number of vascular sources hampers the recruitment of macrophages and T cells leaving microglia as the predominant phagocyte, which are unable to contain the infection due to the absence of lymphocytes. A high degree of vascularization results in clearance of bacteria and increased influx of immune cells. In the hyperemic scenario the predominant phagocytes are macrophages. Although a large number of sources are available, there is no

hyperinflammation as seen in Figure 6c. From this we may conclude that hyperemia does not result in hyperinflammation, indicating that the latter is predominantly driven by TNF-$\alpha$ levels.

## 5. Discussion

Here, we present a novel agent-based model capturing the immune response to Mtb in the brain. Our model not only recapitulates the three major outcomes of tuberculosis namely clearance, containment and uncontrolled growth, but also includes an important fourth outcome of TBM: hyperinflammation, which is known to be associated with severe neurological damage [32]. Our model shows that in order to contain infection without excessive inflammation, an optimal level of TNF-$\alpha$ must be attained. In Figures 5 and 6 both low and high TNF-$\alpha$ levels are detrimental to the host resulting in bacterial overgrowth (Figure 6a) and hyperinflammation (Figure 6c), respectively. Intermediate levels of TNF-$\alpha$ lead to the formation of a stable granuloma containing and controlling the infection. In addition, we find that the amount of available vascular sources influences granuloma development.

### 5.1. What is the optimal TNF level to achieve a stable granuloma?

In humans, primates and mice, TNF-$\alpha$ is essential to the formation, structure and maintenance of a granuloma [29]. TNF-$\alpha$-depleted zebrafish develop granulomas but are unable to maintain the structure and unable to control bacterial growth [51]. Our findings are in line with these animal studies: different TNF-$\alpha$ levels all result in the formation of granuloma, their composition and structure vary however. It is of great interest to understand human genetic susceptibility for TBM. This susceptibility was already shown for the Toll-like receptor pathway in both meningeal and pulmonary TB [52]. More recently, heterozygosity at two intragenic LTA4H single nucleotide polymorphisms protects individuals against pulmonary and meningeal TB in a case control study of Vietnamese TB patients. Strikingly, the same protective effect of heterozygosity was observed for a death outcome in meningeal TB. The LTA4H polymorphisms result in different baseline response levels of TNF-$\alpha$[16, 17]. From a clinical point of view, if this baseline response level of TNF-$\alpha$ is too low then additional inhibition by immunomodulatory drugs may have an adverse effect resulting in uncontrolled bacterial growth. On the other hand, withholding immunomodulatory drugs to patients with abundant levels of TNF-$\alpha$, may result in persisting hyperinflammation with poor outcome also. The optimal TNF-$\alpha$ level is thus reached by taking the baseline TNF-$\alpha$ response level into account as indicated by the patient's genotype. Therefore a randomized clinical trial using immunomodulatory drugs that stratifies for these different genotypes is of great interest. Future work using modeling can explore this further to better predict clinical trial parameters for success, and ruling out those that are unlikely to be successful.

### 5.2. What is the role of immunomodulatory drugs?

Treatment of TBM involves tuberculostatic drugs that interfere with bacterial growth and immunomodulatory drugs that inhibit excessive inflammation. Dexamethasone is a widely used immunomodulatory drug, which downregulates microglia and lymphocytes by inhibiting secretion of several chemokines (CCL2, CCL5, CXCL8, CXCL10) and cytokines (TNF-$\alpha$, IL-1$\beta$, IL-6) *in vitro* [32]. Simmons et al. [53] were unable to show that dexamethasone affects CSF (e.g. TNF-$\alpha$ levels) or blood immune responses in TBM patients. However, a later study showed that dexamethasone is able to influence matrix metalloproteinases [54], which play a role in collagen breakdown and cerebral tissue damage. Also, in TBM patients, dexamethasone has shown to be effective in early stage TBM improving survival and neurological sequelae when used in conjuction with

tuberculostatic drugs [55, 56, 57]. Therefore, WHO recommends dexamethasone as standard therapy for TBM in both children and adults.

Thalidomide is another immunomodulatory drug that targets TNF-$\alpha$[34]. In a rabbit model, the combined use of thalidomide with antibiotics resulted in a reduction in TNF levels and higher survival rate, suggesting a potential clinical role [58]. Nevertheless, a randomized study among children with TBM showed no beneficial effect of thalidomide [59]. This study was terminated prematurely due to adverse effects in the treatment group, which may be attributed to the used dose of thalidomide. Monoclonal antibodies that completely and specifically inhibit TNF-$\alpha$ (e.g. infliximab) are being used for inflammatory bowel disease and rheumatic disorders in children. Because anti-TNF-$\alpha$ antibodies completely remove TNF-$\alpha$, a therapeutical role in TBM is not to be expected. Even more so, its use may lead to reactivation of latent TB [60]. For this reason all children that will be treated with infliximab are screened for latent TB.

**5.3. What is the role of vascularization?—**Among the several pathologic processes that contribute to brain damage in TBM, cerebral infarction plays a major role in the long-term morbidity. The incidence of infarction in TBM ranges from 13% to 53%, the higher incidence being mainly reported in studies involving younger or more severely affected cohorts of children [61]. Beside vascilitis, hypercoagulabilty is a risk factor for thrombosis and stroke in children with TBM. Low and high dose aspirin during the first months of TBM treatment did not improve motor or cognitive outcome in children with advanced TBM [62]. Still it would be of great interest to study the multifactorial pathogenesis of arterial ischemic stroke in TBM. Our model shows that impairment of the amount of vascular sources, which can be used as a proxy for stroke, leads to caseous necrotic granuloma while abundant vascular sources result in clearance of bacteria without hyperinflammation. This might indicate that during TBM development ischemia might further lead to progression of disease in terms of bacterial load and granuloma formation.

### 5.4. Final remarks

The computational model of TBM discussed herein highlights the importance of TNF-$\alpha$ and identified mechanims that potential therapeutic promise. A more detailed model including additional cytokines and chemokines and their mechanisms will likely uncover deeper layers of this complex system. We are currently extending the model to a multi-scale model allowing the study of therapeutical effects of dexamethasone and vitamin D [63] over multiple biological spatial scales, including molecular, intracellular and cellular scales added to the tissue scale model already in place. Similar work has been done for TNF-$\alpha$ in other studies [23].

## Supplementary Material

Refer to Web version on PubMed Central for supplementary material.

## References

1. World Health Organization. 2011/2012 tuberculosis global facts. 2011
2. World Health Organization. Global tuberculosis control 2011. 2011
3. United Nations. 2015 millenium development goals. 2011
4. Zhang M, Gong J, Lin Y, Barnes P. Growth of virulent and avirulent Mycobacterium tuberculosis strains in human macrophages. Infect Immun. 1998; 66(2):794–799. [PubMed: 9453643]
5. Nicas M, Nazaroff WW, Hubbard A. Toward understanding the risk of secondary airborne infection: emission of respirable pathogens. J Occup Environ. 2005; 2(3):143–154.

6. Behr M, Warren S, Salamon H, Hopewell P, de Leon AP, Daley C, Small P. Transmission of Mycobacterium tuberculosis from patients smear-negative for acid-fast bacilli. Lancet. 1999; 353(9151):444–449. [PubMed: 9989714]
7. Krishnan N, Robertson BD, Thwaites G. The mechanisms and consequences of the extra-pulmonary dissemination of mycobacterium tuberculosis. Tuberculosis. 2010; 90(6):361–366. [PubMed: 20829117]
8. Carrol E, Clark J, Cant A. Non-pulmonary tuberculosis. Paediatr Respir Rev. 2001; 2(2):113–119. [PubMed: 12531057]
9. Golden MP, Vikram HR. Extrapulmonary tuberculosis: An overview. Am Fam Physician. 2005; 72(9):1761–1768. [PubMed: 16300038]
10. Forssbohm M, Zwahlen M, Loddenkemper R, Rieder HL. Demographic characteristics of patients with extrapulmonary tuberculosis in germany. Eur Respir J. 2008; 31(1):99–105. [PubMed: 17804450]
11. Rock RB, Olin M, Baker CA, Molitor TW, Peterson PK. Central nervous system tuberculosis: Pathogenesis and clinical aspects. Clin Microbiol Rev. 2008; 21(2):243–261. [PubMed: 18400795]
12. van Well GTJ, Paes BF, Terwee CB, Springer P, Roord JJ, Donald PR, van Furth AM, Schoeman JF. Twenty years of pediatric tuberculous meningitis: A retrospective cohort study in the western cape of south africa. Pediatrics. 2009; 123:e1–e8. [PubMed: 19367678]
13. Barry CE 3rd, Boshoff HI, Dartois V, Dick T, Ehrt S, Flynn J, Schnappinger D, Wilkinson RJ, Young D. The spectrum of latent tuberculosis: rethinking the biology and intervention strategies. Nat Rev Microbiol. 2009; 7(12):845–855. [PubMed: 19855401]
14. Rich A, McCordock H. The pathogenesis of tuberculous meningitis. Bull Johns Hopkins Hosp. 1933; 52:2–37.
15. Tsenova L, Bergtold A, Freedman VH, Young RA, Kaplan G. Tumor necrosis factor $\alpha$ is a determinant of pathogenesis and disease progression in mycobacterial infection in the central nervous system. Proc Natl Acad Sci. 1999; 96:5657–5662. [PubMed: 10318940]
16. Tobin DM, V JC Jr, Ray JP, Walsh GS, Dunstan SJ, Bang ND, Hagge DA, Khadge S, King M-C, Hawn TR, Moens CB, Ramakrishnan L. The lta4h locus modulates susceptibility to mycobacterial infection in zebrafish and humans. Cell. 2010; 140(5):717–730. [PubMed: 20211140]
17. Tobin D, Roca F, Oh S, McFarland R, Vickery T, Ray J, Ko D, Zou Y, Bang N, Chau T, Vary J, Hawn T, Dunstan S, Farrar J, Thwaites G, King MC, Serhan C, Ramakrishnan L. Host genotype-specific therapies can optimize the inflammatory response to mycobacterial infections. Cell. 2012; 148(3):434–446. [PubMed: 22304914]
18. Ramakrishnan L. Revisiting the role of the granuloma in tuberculosis. Nat Rev Immunol. 2012; 12:352–366. [PubMed: 22517424]
19. Be NA, Kim KS, Bishai WR, Jain SK. Pathogenesis of central nervous system tuberculosis. Curr Mol Med. 2009; 9:94–99. [PubMed: 19275620]
20. Jain S, Paul-Satyaseela M, Lamichhane G, Kim K, Bishai W. Mycobacterium tuberculosis invasion and traversal across an in vitro human blood-brain barrier as a pathogenic mechanism for central nervous system tuberculosis. J Infect Dis. 2006; 193(9):1287–1295. [PubMed: 16586367]
21. Ray JCJ, Flynn JL, Kirschner DE. Synergy between individual TNF-dependent functions determines granuloma performance for controlling mycobacterium tuberculosis infection. J Immunol. 2009; 182:3706–3717. [PubMed: 19265149]
22. Marino S, El-Kebir M, Kirschner D. A hybrid multi-compartment model of granuloma formation and t cell priming in tuberculosis. Journal of Theoretical Biology. 2011; 280(1):50–62. [PubMed: 21443879]
23. Fallahi-Sichani M, El-Kebir M, Marino S, Kirschner DE, Lin-derman JJ. Multiscale computational modeling reveals a critical role for tnf-$\alpha$ receptor 1 dynamics in tuberculosis granuloma formation. J Immunol. 2011; 186:3472–3483. [PubMed: 21321109]
24. Cassot F, Lauwers F, Fouard C, Prohaska S, Lauwers-Cances V. A novel three-dimensional computer-assisted method for a quantitative study of microvascular networks of the human cerebral cortex. Microcirculation. 2006; 13:1–18. [PubMed: 16393942]
25. Carson MJ, Doose JM, Melchior B, Schmid CD, Ploix CC. CNS immune privilege: hiding in plain sight. Immunol Rev. 2006; 213(1):48–65. [PubMed: 16972896]

26. Galea I, Bechmann I, Perry VH. What is immune privilege (not)? Trends Immunol. 2007; 28(1): 12–18. [PubMed: 17129764]
27. Polfliet MMJ, Zwijnenburg PJG, van Furth AM, van der Poll T, D¨opp EA, de Lavalette CR, van Kesteren-Hendrikx EML, van Rooijen N, Dijkstra CD, van den Berg TK. Meningeal and perivascular macrophages of the central nervous system play a protective role during bacterial meningitis. J Immunol. 2001; 167:4644–4650. [PubMed: 11591794]
28. van Furth R, Diesselhoff-den Dulk MMD, Mattie H. Quantitative study on the production and kinetics of mononuclear phagocytes during an acute inflammatory reaction. J Exp Med. 1973; 186(6):1314–1330. [PubMed: 4762549]
29. Rock RB, Gekker G, Hu S, Sheng WS, Cheeran M, Lokensgard JR, Peterson PK. Role of microglia in central nervous system infections. Clin Microbiol Rev. 2004; 17(4):942–964. [PubMed: 15489356]
30. Peterson, PK.; Gekker, G.; Hu, S.; Chao, CC. Microglia: A double-edged sword. In: Peterson, PK.; Remmington, JS., editors. Defense of the Brain: Current Concepts in the Immunopathogenesis and Clinical Aspects of Central Nervous System Infections. 1997. p. 31-55.
31. Aloisi F. Immune function of microglia. Glia. 2001; 36(2):165–179. [PubMed: 11596125]
32. Rock RB, Hu S, Gekker G, Sheng WS, May B, Kapur V, Peterson PK. Mycobacterium tuberculosis induced cytokine and chemokine expression by human microglia and astrocytes: Effects of dexamethasone. J Infect Dis. 2005; 192(12):2054–2058. [PubMed: 16288367]
33. Abdallah AM, Bestebroer J, Savage NDL, de Punder K, van Zon M, Wilson L, Korbee CJ, van der Sar AM, Ottenhoff THM, van der Wel NN, Bitter W, Peters PJ. Mycobacterial secretion systems esx-1 and esx-5 play distinct roles in host cell death and inflammasome activation. J Immunol. 2011; 187(9):4744–4753. [PubMed: 21957139]
34. Peterson PK, Hu S, Sheng WS, Kravitz FH, Molitor TW, Chatterjee D, Chao CC. Thalidomide inhibits tumor necrosis factor-alpha production by lipopolysaccharide- and lipoarabinomannan-stimulated human microglial cells. J Infect Dis. 1995; 172(4):1137–1140. [PubMed: 7561198]
35. O'Garra A, Vieira PL, Vieira P, Goldfeld AE. IL-10-producing and naturally occurring CD4+ Tregs: limiting collateral damage. J Clin Invest. 2004; 114:1372–1378. [PubMed: 15545984]
36. Marino, S.; Fallahi-Sichani, M.; Linderman, JJ.; Kirschner, DE. Mathematical Models of Anti-TNF Therapies and their Correlation with Tuberculosis. John Wiley & Sons, Inc.; 2012. p. 83-104.
37. Flynn JL, Goldstein MM, Chan J, Triebold KJ, Pfeffer K, Lowenstein CJ, Schrelber R, Mak TW, Bloom BR. Tumor necrosis factor-$\alpha$ is required in the protective immune response against mycobacterium tuberculosis in mice. Immunity. 1995; 2(6):561–572. [PubMed: 7540941]
38. Capuano SV, Croix DA, Pawar S, Zinovik A, Myers A, Lin PL, Bissel S, Fuhrman C, Klein E, Flynn JL. Experimental mycobacterium tuberculosis infection of cynomolgus macaques closely resembles the various manifestations of human m. tuberculosis infection. Infect Immun. 2003; 71(10):5831–5844. [PubMed: 14500505]
39. Lin P, Rodgers M, Smith L, Bigbee M, Myers A, Bigbee C, Chiosea I, Capuano S, Fuhrman C, Klein E, Flynn J. Quantitative comparison of active and latent tuberculosis in the cynomolgus macaque model. Infect Immun. 2009; 77(10):4631–4642. [PubMed: 19620341]
40. Keane J, Gershon S, Wise RP, Mirabile-Levens E, Kasznica J, Schwieterman WD, Siegel JN, Braun MM. Tuberculosis associated with infliximab, a tumor necrosis factor neutralizing agent. New Engl J Med. 2001; 345(15):1098–1104. [PubMed: 11596589]
41. Iliopoulos A, Psathakis K, Aslanidis S, Skagias L, Sfikakis P. Tuberculosis and granuloma formation in patients receiving anti-tnf therapy. Int J Tuberc Lung D. 2006; 10(5):588–590.
42. Bonabeau E. Agent-based modeling: methods and techniques for simulating human systems. Proc Nat Acad Sci. 2002; 99(Suppl. 3):7280–7287. [PubMed: 12011407]
43. Landreth GE. Microglia in central nervous system diseases. J Neuroimmune Pharmacol. 2009; 4:369–370. [PubMed: 19763835]
44. Lawson L, Perry V, Gordon S. Turnover of resident microglia in the normal adult mouse brain. Neuroscience. 1992; 48:405–415. [PubMed: 1603325]
45. Ray JCJ, Wang J, Chan J, Kirschner DE. The timing of tnf and ifn-gamma signaling affects macrophage activation strategies during mycobacterium tuberculosis infection. J Theor Biol. 2008; 252(1):24–38. [PubMed: 18321531]

46. Kauppinen TM, Swanson RA. Poly polymerase-1 promotes microglial activation, proliferation, and matrix metalloproteinase-9-mediated neuron death. J Immunol. 2005; 174(4):2288–2296. [PubMed: 15699164]
47. Shankaran M, Marino ME, Busch R, Keim C, King C, Lee J, Killion S, Awada M, Hellerstein MK. Measurement of brain microglial proliferation rates in vivo in response to neuroinflammatory stimuli: Application to drug discovery. J Neurosci Res. 2007; 85(11):2374–2384. [PubMed: 17551981]
48. Huse M, Lillemeier BF, Kuhns MS, Chen DS, Davis MM. T cells use two directionally distinct pathways for cytokine secretion. Nat Immunol. 2006; 7:247–55. [PubMed: 16444260]
49. El-Kebir, M. Master's Thesis. VU University Amsterdam, Faculty of Sciences; Aug. 2010 Modeling Tuberculosis In Lung And Central Nervous System.
50. Marino S, Hogue IB, Ray CJ, Kirschner DE. A methodology for performing global uncertainty and sensitivity analysis in systems biology. J Theor Biol. 2008; 254:178–196. [PubMed: 18572196]
51. Clay H, Volkman HE, Ramakrishnan L. Tumor necrosis factor signaling mediates resistance to mycobacteria by inhibiting bacterial growth and macrophage death. Immunity. 2008; 29(2):283–294. [PubMed: 18691913]
52. Hawn TR, Dunstan SJ, Thwaites GE, Simmons CP, Thuong NT, Lan NTN, Quy HT, Chau TTH, Hieu NT, Rodrigues S, Janer M, Zhao LP, Hien TT, Farrar JJ, Aderem A. A polymorphism in toll-interleukin 1 receptor domain containing adaptor protein is associated with susceptibility to meningeal tuberculosis. J Infect Dis. 2006; 194(8):1127–1134. [PubMed: 16991088]
53. Simmons CP, Thwaites GE, Quyen NTH, Chau TTH, Mai PP, Dung NT, Stepniewska K, White NJ, Hien TT, Farrar J. The clinical benefit of adjunctive dexamethasone in tuberculous meningitis is not associated with measurable attenuation of peripheral or local immune responses. J Immunol. 2005; 175(1):579–590. [PubMed: 15972695]
54. Green JA, Tran CTH, Farrar JJ, Nguyen MTH, Nguyen PH, Dinh SX, Ho NDT, Ly CV, Tran HT, Friedland JS, Thwaites GE. Dexamethasone, cerebrospinal fluid matrix metalloproteinase concentrations and clinical outcomes in tuberculous meningitis. PLoS ONE. 2009; 4(9):e7277. [PubMed: 19789647]
55. Prasad K, Singh MB. Corticosteroids for managing tuberculous meningitis. Cochrane Db Syst Rev. 2009; (1)
56. Thwaites GE, Bang ND, Dung NH, Quy HT, Oanh DTT, Thoa NTC, Hien NQ, Thuc NT, Hai NN, Lan NTN, Lan NN, Duc NH, Tuan VN, Hiep CH, Chau TTH, Mai PP, Dung NT, Stepniewska K, White NJ, Hien TT, Farrar JJ. Dexamethasone for the treatment of tuberculous meningitis in adolescents and adults. New Engl J Med. 2004; 351(17):1741–1751. [PubMed: 15496623]
57. Torok ME, Bang ND, Chau TTH, Yen NTB, Thwaites GE, Quy H Thi, Dung NH, Hien TT, Chinh NT, Thanh Hoang H Thi, Wolbers M, Farrar JJ. Dexamethasone and long-term outcome of tuberculous meningitis in vietnamese adults and adolescents. PLoS ONE. 2011; 6(12):e27821. [PubMed: 22174748]
58. Tsenova L, Sokol K, Freedman VH, Kaplan G. A combination of thalidomide plus antibiotics protects rabbits from mycobacterial meningitis-associated death. J Infect Dis. 1998; 177(6):1563–1572. [PubMed: 9607834]
59. Schoeman JF, Springer P, van Rensburg AJ, Swanevelder S, Hanekom WA, Haslett PAJ, Kaplan G. Adjunctive thalidomide therapy for childhood tuberculous meningitis: Results of a randomized study. J Child Neurol. 2004; 19(4):250–257. [PubMed: 15163089]
60. Fallahi-Sichani M, Flynn JL, Linderman JJ, Kirschner DE. Differential risk of tuberculosis reactivation among anti-tnf therapies is due to drug binding kinetics and permeability. J Immunol. 2012; 188(7):3169–3178. [PubMed: 22379032]
61. Schoeman J, Mansvelt E, Springer P, van Rensburg AJ, Carlini S, Fourie E. Coagulant and Fibrinolytic Status in Tuberculous Meningitis. Pediatr Infect Dis J. 2007; 26(5):428–431. [PubMed: 17468654]
62. Schoeman JF, van Rensburg A Janse, Laubscher JA, Springer P. The role of aspirin in childhood tuberculous meningitis. J Child Neurol. 2011; 26(8):956–962. [PubMed: 21628697]
63. Visser DH, Schoeman JF, Van Furth AM. Seasonal variation in the incidence rate of tuberculous meningitis is associated with sunshine hours. Epidemiol Infect. 2012 Epub ahead of print.

## Highlights

- We introduce an in silico model capturing the immune response to Mtb in the brain.
- We show there is a dose-dependent effect of TNF on bacterial load and tbm onset.
- We show that impairment of cerebral blood flow leads to a higher bacterial load.

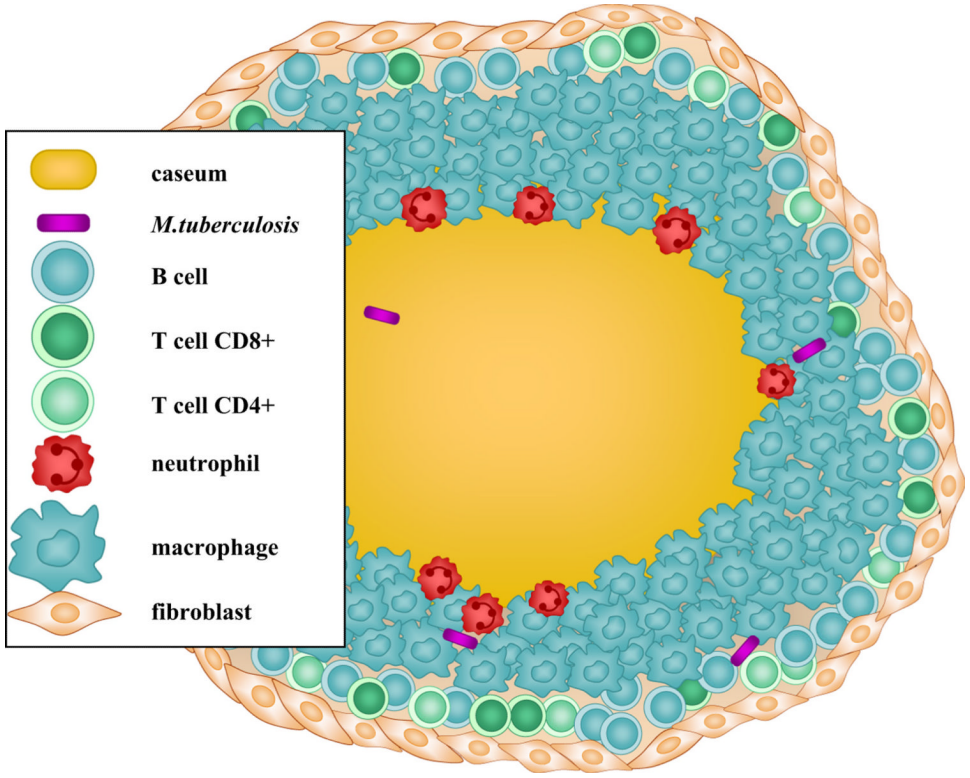


**Figure 1.**
A granuloma is a spherical structure consisting of a necrotic caseating core surrounded by a several types of immune cells.

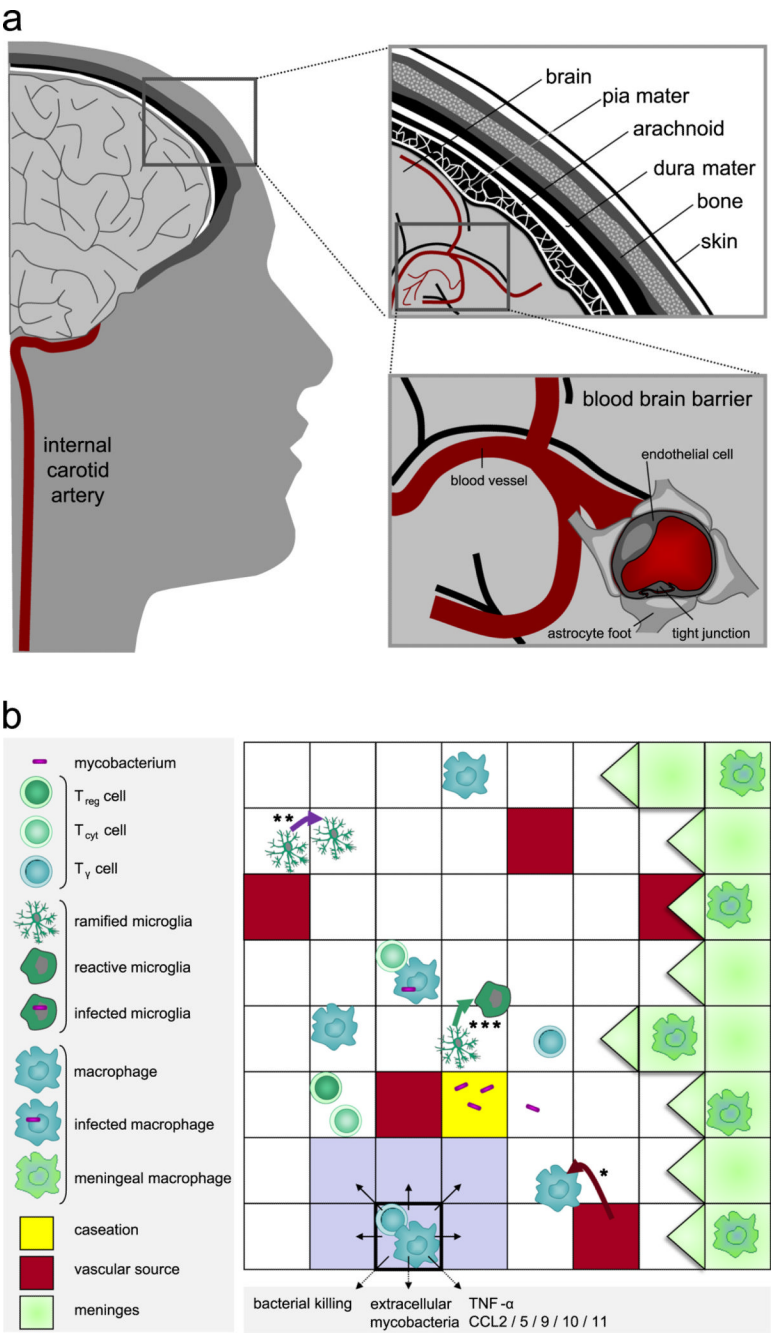


**Figure 2.**

Brain environment. (a) Environment of TBM. The right upper panel shows a cross-section of brain, meninges, skull and skin. The right lower panel shows cerebral blood vessels with a detail of the blood-brain barrier: the blood vessel wall consists of closely-connected endothelial cells resulting in tight junctions that are supported by astrocytes. (b) Environment of the granuloma showing a part of the 10,000 micro-compartments grid. In the panel different immune cells, bacteria and static properties of the grid are depicted. Macrophages and T cells enter the grid through vascular sources (*). Microglia proliferate on site (**). Example of microglia state transition from ramified to reactive (***). The Moore neighborhood of the micro-compartment with highlighted borders is colored in gray.

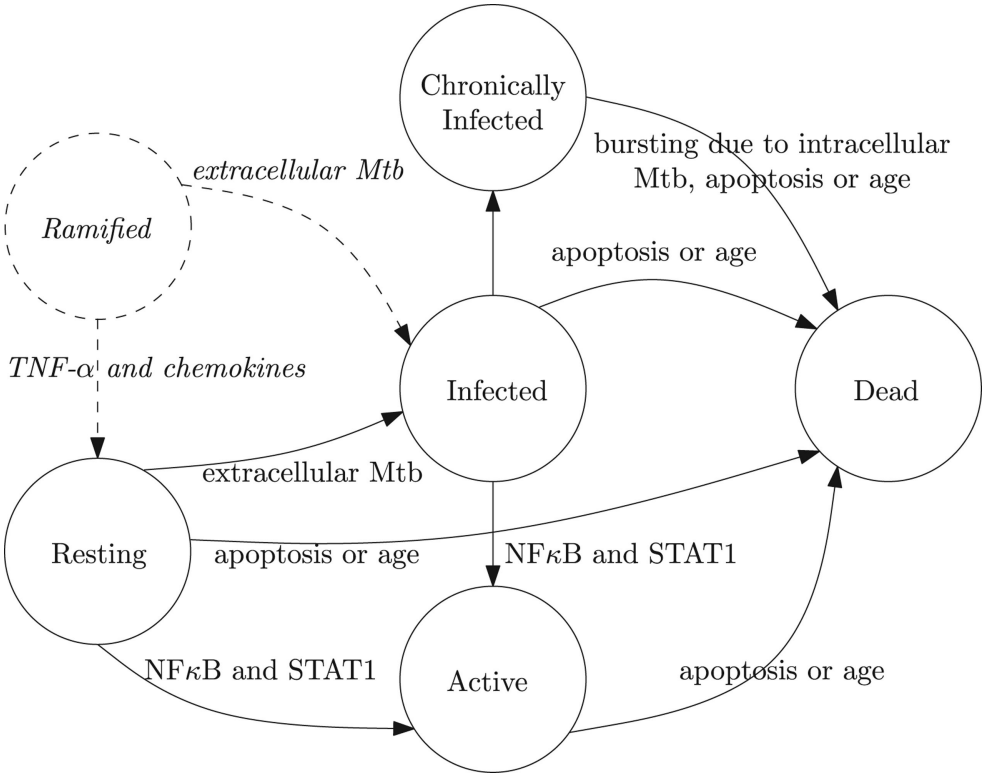


**Figure 3.**
State transitions of phagocytes. Dashed states and transitions are specific to microglia.

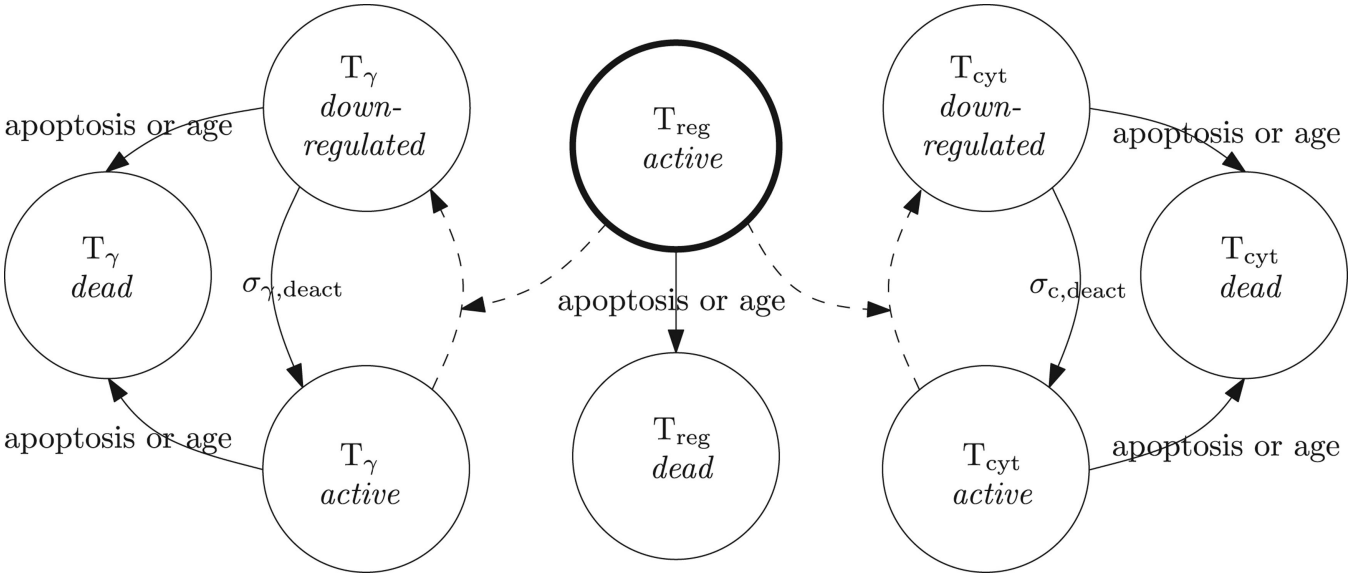


**Figure 4.**
State transitions of T cells. Dashed arrows correspond to down-regulation by $T_{reg}$ cells.

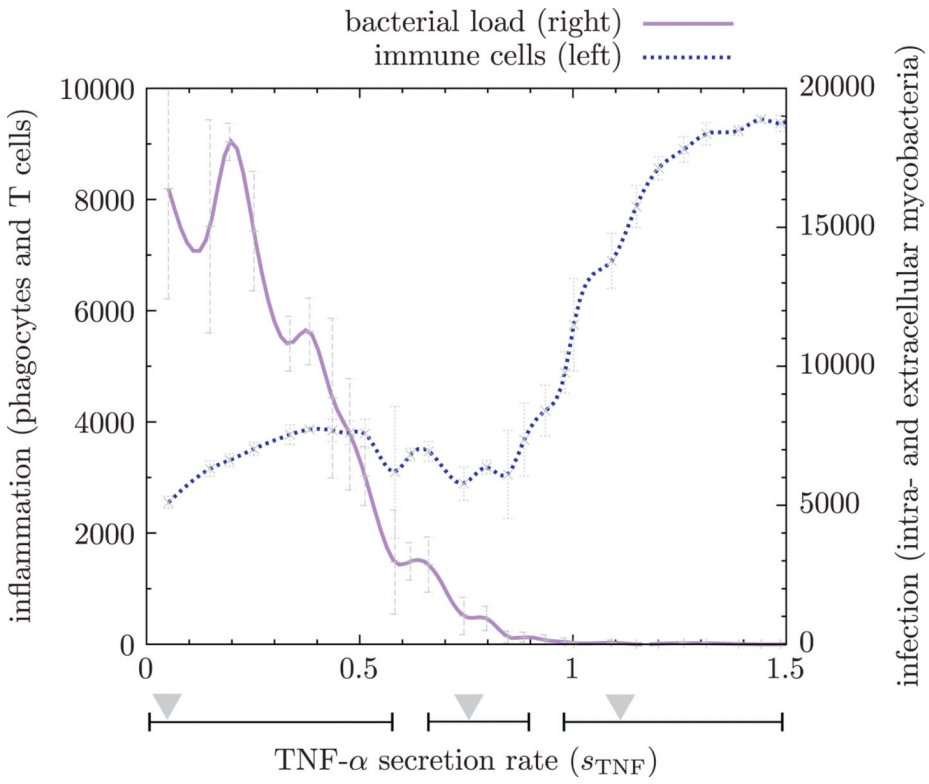


**Figure 5.**

Dose-dependent response of TNF-$\alpha$ secretion rate on bacterial load and immune cell numbers. Too little TNF-$\alpha$ results in uncontrolled bacterial growth; the interval of this phenomenon is shown by the leftmost horizontal bar under the graph where the triangle indicates $s_{\mathrm{P,TNF}} = 0.1$ corresponding to Figure 6a. The second horizontal bar denotes intermediate levels of TNF-$\alpha$ resulting in containmnent/clearance as shown in Figure 6b. The second triangle corresponds to the baseline containment scenario where $s_{\mathrm{P,TNF}} = 0.7$. The third bar shows high levels of TNF-$\alpha$ which do lead to clearance as well as harmful hyperinflammation (see Figure 6c, triangle at $s_{\mathrm{P,TNF}} = 1.1$). Vertical error bars indicate standard deviations of $n = 5$ repetitions.

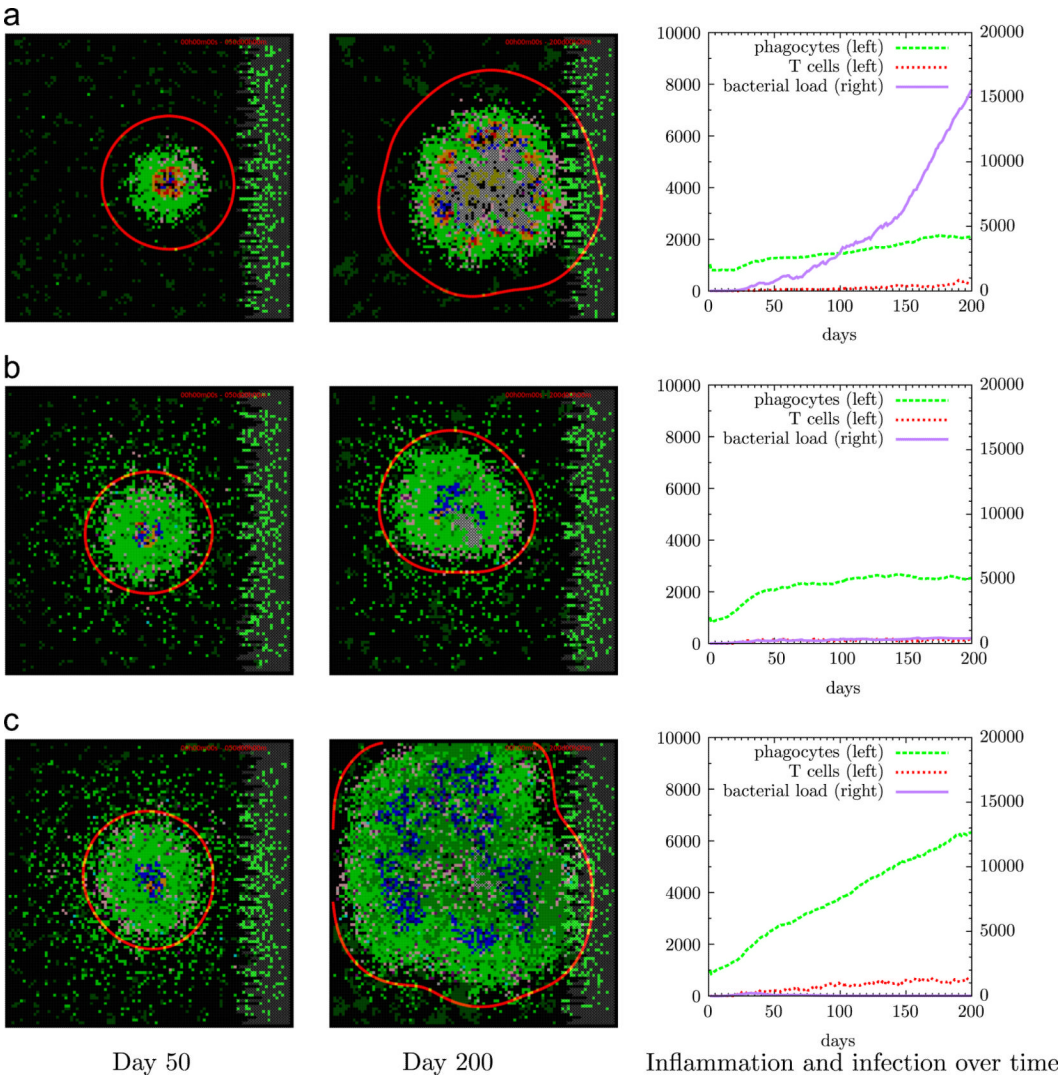


**Figure 6.**

Three TNF-$\alpha$ secretion-rate scenarios (A–C). First two columns show snapshots of the grid at days 50 and 200, third column shows numbers of bacteria and immune cells over time. Scenario A (uncontrolled bacterial growth, $s_{P,TNF} = 0.1$) shows scattered ramified microglia in dark green and bacteria at the center in brown together with infected phagocytes in yellow and red, and a substantial amount of caseation in grey. Scenario B (containment, $s_{P,TNF} = 0.7$) shows a stable granuloma with a core of little caseation and infected (red) and activated (blue) phagocytes surrounded by resting phagocytes (green) and a rim of T cells (purple and pink). Scenario C (hyperinflammation, $s_{P,TNF} = 1.1$) shows high numbers of phagocytes and lymphocytes in the absence of bacteria. Time-lapse movies of these scenarios can be found in the supplementary information.

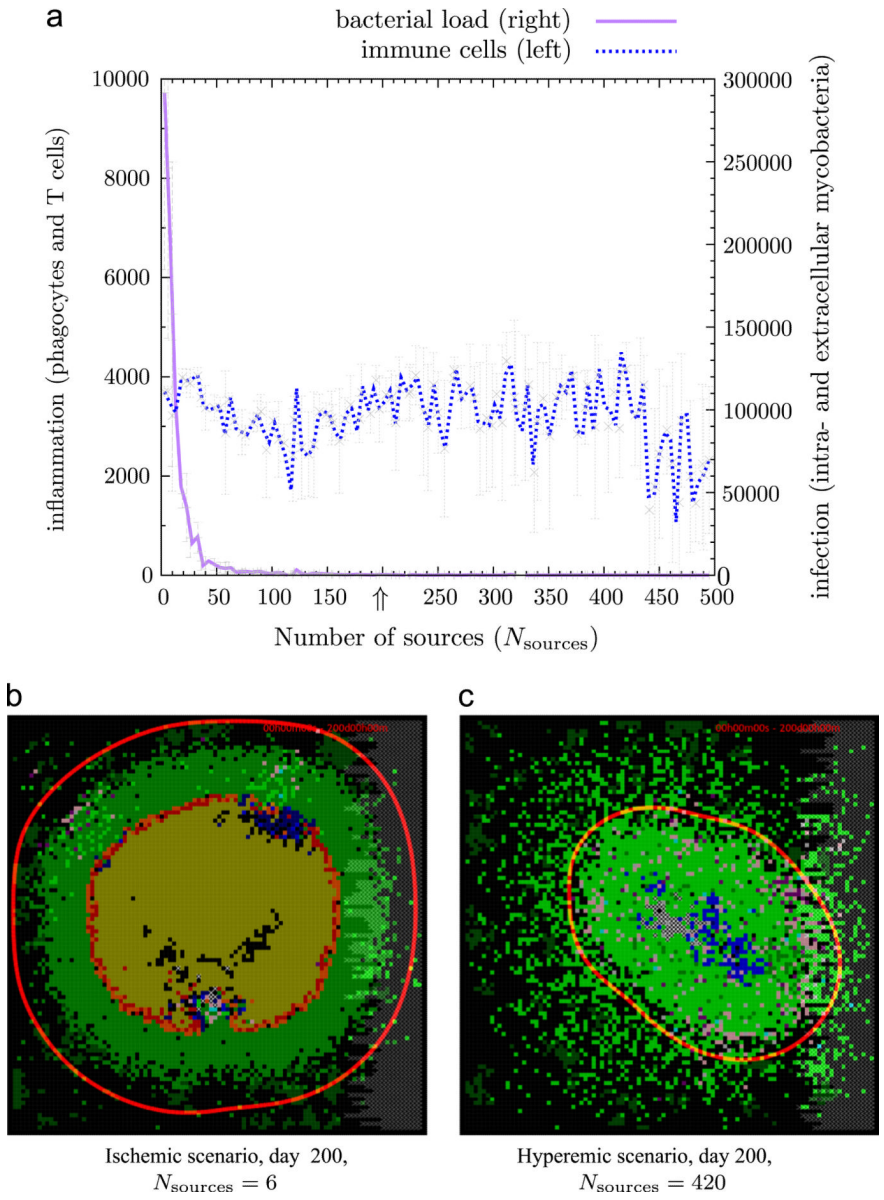


**Figure 7.**

Effect of vascularization on bacterial load and immune cell numbers. A low number of vascular sources hampers the recruitment of macrophages and T cells leaving microglia as the predominant phagocyte, which are unable to contain the infection resulting in the formation of pus as shown in (b). A high degree of vascularization results in clearance of bacteria and increased influx of immune cells as shown in (c). In the hyperemic scenario the predominant phagocytes are macrophages. Figure 8 shows how phagocyte and lymphocyte numbers develop over time in both scenarios. The arrow at $N_{\text{sources}} = 200$ indicates our baseline containment scenario. All experiments were performed using the baseline containment scenario (Supplementary Table 1) with intermediate TNF-$\alpha$ levels. Time-lapse movies of these two scenarios can be found in the supplementary information.

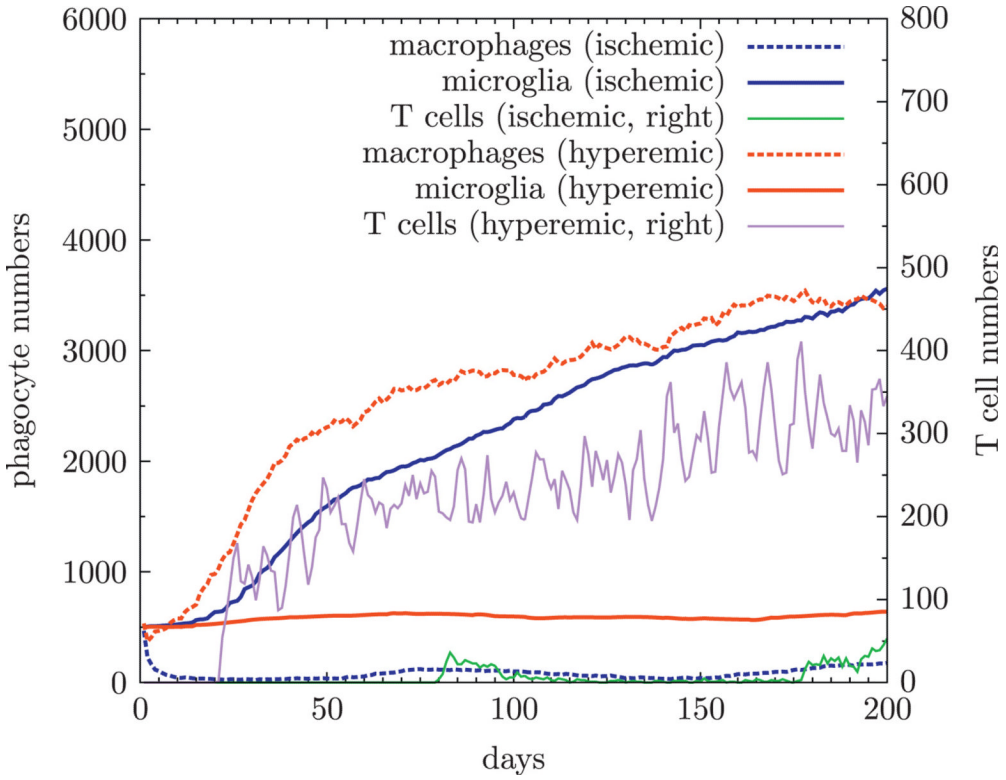


**Figure 8.**
Development of phagocytes and lymphocytes over time in hyperemic and ischemic states. During ischemia recruitment of macrophages and lymphocytes is hampered as is reflected by low macrophage and lymphocyte number. This is not the case during hyperemia, macrophage numbers increase as infection develops (lowest two lines). In the absence of macrophages during ischemia, microglia proliferate reaching the same numbers as macrophages do in hyperemia.

## Table 1

LHS results showing for every parameter the partial-rank correlation coefficient between bacterial load (only PRCC values with a $p$ value less than 0.0001 are considered).

| Parameter | Description | LHS range | PRCC |
|---|---|---|---|
| $s_{P,TNF}$ | Maximal number of TNF-$\alpha$ molecules that a phagocyte can secrete every 6-second time step | [0, 2.5] | −0.67 |
| $p_{T,P}$ | Probability of moving a T cell onto a micro-compartment containing a phagocyte | [0.005, 0.05] | −0.61 |
| $p_{T,recr}$ | Probability of recruiting a T cell | [0.05, 0.3] | −0.40 |
| $\tau_{P,TNF,NF\kappa B}$ | TNF-$\alpha$ level required for NF$\kappa$B activation in phagocytes | [0.01, 0.1] | 0.36 |
| $p_{M,recr}$ | Probability of recruiting a macrophage | [0.01, 0.1] | 0.32 |
| $N_{caseous}$ | Number of killings for a microcompartment to become caseous | [5, 15] | −0.23 |
| $p_{T,T}$ | Probability of moving a T cell onto a micro-compartment already containing a T cell | [0.01, 0.1] | −0.21 |